Environ. Eng. Res. 2019; 24(3): 474-483
https://doi.org/10.4491/eer.2018.232

pISSN 1226-1025
eISSN 2005-968X

Removal of toxic hydroquinone: Comparative studies on use of iron impregnated granular activated carbon as an adsorbent and catalyst

Ankit Tyagi[1], Susmita Das[1,2], Vimal Chandra Srivastava[1†]

[1]*Department of Chemical Engineering, Indian Institute of Technology Roorkee, Roorkee, 247667, Uttarakhand, India*
[2]*Department of Chemical Engineering, National Institute of Technology Calicut, Kozhikode, Kerala 673 601, India*

ABSTRACT

In this study, iron (Fe) impregnated granular activated carbon (Fe-GAC) has been synthesized and characterized for various properties. Comparative studies have been performed for use of Fe-GAC as an adsorbent as well as a catalyst during catalytic oxidation of hydroquinone (HQ). In the batch adsorption study, effect of process parameter like initial HQ concentration (C_o = 25-1,000 mg/L), pH (2-10), contact time (t: 0-24 h), temperature (T: 15-45°C) and adsorbent dose (w: 5-50 g/L) have been studied. Maximum HQ adsorption efficiency of 75% was obtained at optimum parametric condition of: pH = 4, w = 40 g/L and t = 14 h. Pseudo-second order model best-fitted the HQ adsorption kinetics whereas Langmuir model best-represented the isothermal equilibrium behavior. During oxidation studies, effect of various process parameters like initial HQ concentration (C_o: 20-100 mg/L), pH (4-8), oxidant dose (C_{H2O2}: 0.4-1.6 mL/L) and catalyst dose (m: 0.5-1.5 g/L) have been optimized using Taguchi experimental design matrix. Maximum HQ removal efficiency of 83.56% was obtained at optimum condition of C_o = 100 mg/L, pH = 6, C_{H2O2} = 0.4 mL/L, and m = 1 g/L. Overall use of Fe-GAC during catalytic oxidation seems to be a better as compared to its use an adsorbent for treatment of HQ bearing wastewater.

Keywords: Adsorption, Catalytic oxidation, Granular activated carbon, Hydroquinone, Taguchi methodology

1. Introduction

Hydroquinone (HQ) is one the most harmful benzene metabolite phenolic organic compound which has been found in the effluent of various industries [1, 2]. HQ has several toxic effects on the environment, animal as well as human health. It is very toxic to aquatic organism, shellfish and fish at the concentration levels of parts-per-million. It is the most toxic dihydroxybenzene which decreases the cultivable microorganisms with increasing concentration [2]. At higher dose of HQ, malformation in chick embryos is reported [3]. HQ has toxic effect on human lymphocytes by inducing apoptosis by activating caspases 9/3 pathway [4]. Oral administration of HQ to fasting animal can cause death within few minutes, and repeated exposure to HQ can cause tremors and clonic seizures, paralysis of respiratory systems of animals [5]. It has inhibitory effect on mouse and human bone marrow cells [6], etc.

Several treatment methods such as fixed bed reactor [7, 8], electrochemical oxidation [9-10], photo-oxidation [11], enzyme catalytic oxidation under bio catalytic micro-reactor [12], oxidation [13], and electro-catalytic oxidation have been used for removal of phenolic compounds such as HQ from aqueous solution. Among all these methods, oxidation is economically and ecologically most promising technique [14] to convert phenolic compound into its harmless intermediates which also show antifungal, antibacterial, antiviral and anticancer activities [13-15]. People have used this technique to remove HQ with different catalyst like: Cu(II)-polyvinyl-imidazole complex, vinyl-imidazole and ethyl-vinyl sulphide copolymers [5, 16-18], polyvinyl-pyridine-Cu(II) complex [19], polymer supported copper catalyst [20], silica supported sulfonic acid [14], silver oxide [21], active carbon or a commercial copper oxide supported over alumina [13], acrylic resin supported Cu(II) [17], etc.

Activated carbons derived from various sources and other carbo-

Received July 11, 2018 **Accepted** November 10, 2018

† Corresponding author
Email: vimalcsr@yahoo.co.in
Tel: +91-1332-285889 Fax: +91-1332-276535
ORCID: 0000-0001-5321-7981

naceous materials have generally been used for the adsorptive removal of various pollutants like phenolic compounds and dyes [22-27]. A number of investigators have previously used iron/iron oxide impregnated activated carbon for treatment of phenolic and other toxic compounds containing aqueous solution [28-35]. Lücking et al. [31] studied oxidation of 4-chlorophenol whereas Zazo et al. [32] and Abussaud et al. [33] studied mineralization of phenol. Yin et al. [34] reviewed enhancement in pollutant removal by modifications of activated carbon. Similarly, Pereira et al. [35] reviewed iron oxide catalysts for mineralization of pollutants. Several mechanisms including non-radical [36] and radical [37, 38] mechanisms have been proposed for the mineralization of pollutants especially organic compounds by iron based catalysts. Although, studies have been performed in the literature on adsorption of HQ by granular activated carbon (GAC), however, studies on adsorption/mineralization of HQ by iron (Fe) impregnated GAC (Fe-GAC) are scarce.

Motivated by the above literature, this research aims to compare the use of Fe-GAC as an adsorbent as well as a catalyst during catalytic oxidation of HQ. Fe-GAC has been prepared by impregnation of Fe over GAC and its physico-chemical and analytical properties have been characterized. These characteristics include scanning electron microscopic (SEM), Fourier transform infrared spectral (FTIR) analysis, Brunauer-Emmett-Teller (BET) surface area, thermogravimetric (TG) analysis, etc. During use of Fe-GAC as an adsorbent in batch adsorption process, effects of various parameters like: initial pH (pH_o), adsorbent dose (w), contact time (t), initial concentration (C_o) and temperature (T) along with the adsorption kinetics and isotherm study have been performed for the HQ removal from the aqueous solution. In the catalytic oxidation process of HQ in batch reactor, effect of various experimental parameters like: catalyst dose (m), oxidant (hydrogen per oxide) dose (C_{H2O2}), C_o and pH_o have been studied. Finally a comparison of adsorption and catalytic oxidation process has been done.

2. Materials and Methods

2.1. Chemicals

Chemicals used for this study were of analytical reagent grade. Ferric nitrate ($Fe(NO_3)_3.9H_2O$) (S. D. Fine Chemicals Limited, India), HQ (Qualigens Fine Chemicals, India), Hydrogen peroxide (H_2O_2) (Rankem Limited, India) and GAC (1-5 mm) (Innova corporate, India) were used for the study.

2.2. Preparation of Fe-GAC and Its Characterization

Fe-GAC catalyst/adsorbent was prepared by the method as reported in the literature [39]. GAC was sieved in size range of 1-5 mm and kept in the muffle furnace at 300℃ for 4 h for moisture removal. 45 g of GAC was mixed with $Fe(NO_3)_3.9H_2O$ solution (36.07 g of $Fe(NO_3)_3.9H_2O$ in 25 mL distilled water) for 10% loading and impregnated for 2 h. Mixture was dried for 12 h in an oven at 60℃ and heated inside the muffle furnace at 200℃ for 4 h. The resultant solid sample obtained, was named as Fe-GAC and it was used in both oxidation as well as adsorption studies.

MAC bulk density apparatus was used for determining the bulk density. Proximate analysis was performed as per bureau of Indian standards [40]. Surface area was determined by using surface area and porosity analyzer (Micromeritics ASAP 2020). X-ray diffraction analysis (XRD) was done by using Bruker AXS, Diffractometer D8, Germany, X-ray diffractometer. International centre for diffraction data (ICDD) library was used to identify the compounds. SEM (QUANTA, Model 200 FEG, Netherlands) was used to capture the morphology of the Fe-GAC. To know the functional groups, KBr pellet method was used to measure the FTIR spectra (Thermo Nicolet 6700, NEXUS, USA) in range of 4,000-400 cm^{-1}. Thermogravimetric analysis (TGA) (EX STAR 6300) was carried out from room temperature to 1,000℃ under air atmosphere, non-isothermally. Moisture-free air flow rate was kept constant at 200 mL/min during the experiment.

2.3. Batch Adsorption Studies

Experiments were carried out in batch mode for studying the effect of parameters like: pH_o, w, C_o, t and T. 100 mL of known concentration HQ solution was added along-with a known quantity of adsorbent within a flask and kept in an orbital shaking incubator (150 rpm) at known temperature (15, 30 or 45℃). Aqueous solution of HCl and NaOH (concentration 0.1 M each) was used to maintain the adsorbate solution pH during the experiment. The resultant solution was centrifuged and residual concentration of HQ was measured. The experiments were performed at various pH (2-10) at C_o = 100 mg/L and w = 10 g/L at 30℃. To find the optimum w, experiments were carried out with different dosage of Fe-GAC (5 to 50 g/L) with C_o = 100 mg/L at 30℃. Kinetic study was done by finding the adsorption uptake of HQ solution (C_o = 25-100 mg/L, w = 40 g/L) at different time intervals over 24 h. Effect of temperature was analyzed by taking varying C_o (25-1,000 mg/L) at different T (15-45℃).

During the studies, the concentration of HQ (λ_{max} = 289 nm) was determined by UV/VIS spectrophotometer (UV 1800, Shimadzu Corporation). Percentage HQ removal was calculated according to Eq. (1).

$$Removal\ efficiency(\%) = 100(C_o - C_e)/C_o \quad (1)$$

where, C_e represents the final concentration of the HQ solution (mg/L). The equilibrium adsorption uptake in solid phase q_e (mg/g) is defined in Eq. (2).

$$Amount\ of\ adsorbed\ HQ\ per\ g\ of\ solid,\ q_e = (C_o - C_e)\,V/w \quad (2)$$

where, V is the volume of the solution (L) and w is the mass of adsorbent (g).

2.4. Catalytic Oxidation Studies

Triple necked glass reactor fitted with a shell and tube type condenser and a magnetic stirrer was used for carrying out the HQ oxidation studies with Fe-GAC as catalysts. The reactor was kept inside an oil bath so as to perform experiment at 50℃ for 4 h. The 3-level 4-factor Taguchi design for experiments was used in the experimental study. C_o: 20-100 mg/L, pH: 4-8, C_{H2O2}: 0.4-1.6 mL/L and m: 0.5-1.5 g/L were the variable input parameters. L_9

Table 1. Process Parameters, Their Levels and HQ Removal Efficiency during Experiments Carried Out as per L_9 Taguchi's Orthogonal Array for Oxidative Treatment Using H_2O_2 as Oxidant and Fe-GAC as Catalyst

Exp. no	Factors or parameters and their values				Removal efficiency (%)
	A: Initial concentration (C_o, mg/L)	B: pH	C: H_2O_2 dose (C_{H2O2}, mL/L)	D: Catalyst dose (m, g/L)	
1	20	4	0.4	0.5	70.35
2	20	6	1	1	81.23
3	20	8	1.6	1.5	75.52
4	60	4	1	1.5	71.32
5	60	6	1.6	0.5	75.25
6	60	8	0.4	1	81.25
7	100	4	1.6	1	72.19
8	100	6	0.4	1.5	84.51
9	100	8	1	0.5	74.46

(3^4) orthogonal array (OA) has been selected for the catalytic oxidation of HQ (Table 1). Experimental data was analyzed as per literature [24-26] with "higher-is-better" quality characteristic using plot of average response curve and ANOVA analysis. The mean at the optimal condition was estimated by Eq. (3).

$$\mu = \overline{T} + (\overline{A} - \overline{T}) + (\overline{B} - \overline{T}) + (\overline{C} - \overline{T}) + (\overline{D} - \overline{T}) = \overline{A} + \overline{B} + \overline{C} + \overline{D} - 3\overline{T} \quad (3)$$

where, $\overline{T}$ represents the overall mean of response, and $\overline{A}$, $\overline{B}$, $\overline{C}$ and $\overline{D}$ are the average value of response at optimum level for parameters A, B, C and D, respectively. Confidence intervals for the population (CI_{POP}) and for confirmation experiments (CI_{CE}) as given in literature [41-43]. Three confirmation experiments were performed at the predicted optimum conditions [44-46].

3. Results and Discussion

3.1. Batch Adsorption Studies

The pH_o effect on the HQ adsorption via Fe-GAC adsorbent was examined with C_o = 100 mg/L, w = 10 g/L, T = 30℃ and t = 10 h. Fig. S1 shows the variation of removal efficiency with pH_o and final pH (pH_f) of the solution. The removal of HQ was maximum at pH_o = 4. The $pK_{a,1}$ and $pK_{a,2}$ values of HQ are found to be 9.9 and 11.6, respectively [46]. HQ forms negatively charged hydroquinate anion and hydroquinate dianions beyond pH 8 and 10, respectively. HQ remains in neutral form for pH ≤ 8 [47]. Fig. S1 also shows that pH_f of the solution increased up to $pH_o \leq 4$ after that it become almost constant. The increase in the pH after adsorption for $pH_o \leq 5.5$ may be due to adsorption of H^+ ions to Fe-GAC. However, for $pH_o \geq 5.5$, OH^- ions compete with HQ anions present in the solution for the adsorption sites present on Fe-GAC. This is also clear from the fact that the pH of the solution increases for all test runs which were conducted at $pH_o \geq 6$. And because of the competitive adsorption of the OH^- ions, HQ removal efficiency decreases at higher pH.

The effect of w on HQ removal efficiency by Fe-GAC is shown in Fig. S2. This figure shows that the HQ removal increased as the w was increased (w < 40 g/L). For w > 40 g/L, HQ saturates the surface of adsorbent, so the solution having large remaining concentration of HQ and removal efficiency was less. Removal efficiency increased with an increase in w for w < 40 g/L because adsorption sites are more at adsorbent surface. For w ≤ 40 g/L, the residual HQ concentration was low and removal efficiency was always high because of the increase in surface area at high amount of adsorbent. However, particle-particle interaction such as aggregation at higher w restricts increase in the surface area of the adsorbent beyond a certain value. Also an increase in the diffusional path length at higher w deters further improvement in the removal efficiency of HQ [48].

The time (t) effect on the HQ adsorption by Fe-GAC was understood by doing experiment for 24 h with C_o = 25-100 mg/L at 30℃. The results are shown in Fig. 1(a). It shows faster adsorption of HQ in first 200 min, after that the adsorption rate becomes almost constant and equilibrium was attained in 14 h contact time. As C_o increased, the adsorption rate also increased for the same t. The uptake of HQ is fast during initial contact period because of the more availability of vacant sites at adsorbent surface for adsorption of HQ. Later adsorption rate becomes slower near the equilibrium as a result of repulsion between the solute molecules on the adsorbent and bulk phases.

In the present study, well-known pseudo-first order and pseudo-second order kinetic models were tried for possible representation of HQ adsorption kinetics onto Fe-GAC [48-51]. Pseudo-second rate constant (ks), equilibrium adsorption capacity (q_e), and initial sorption rate (h) were calculated from the non-linear fitting of experimental data into the rate equations (Fig. 1(a)). Above parameters are shown in Table 2. The kinetic data satisfactorily exhibited pseudo-second order kinetics.

Fig. 1(b) shows Weber-Morris plot of q_t versus $t^{1/2}$ [52] at various C_o of HB adsorption onto Fe-GAC. The bi-linear plot signifies that the adsorption process is being controlled by more than one process. The rate of adsorption in these regions are defined by

Table 2. Kinetic Parameters for the Removal of HQ by Fe-GAC (t = 24 h, C_o = 25-100 mg/L, w = 40 g/L, T = 30°C)

Pseudo-first order model						
C_o (mg/L)	**$q_{e,exp}$ (mg/g)**	**$q_{e,cal}$ (mg/g)**	**k_f (min^{-1})**	**R^2**	**MPSD**	**Chi square (χ^2)**
25	0.260	0.190	0.009	0.942	29.404	0.031
50	0.688	0.629	0.006	0.969	59.457	0.117
100	1.762	1.559	0.010	0.989	37.088	0.104
Pseudo-second order model						
C_o (mg/L)	**$q_{e,cal}$ (mg/g)**	**k_s (g/mg min)**	**h (mg/g min)**	**R^2**	**MPSD**	**Chi square (χ^2)**
25	0.229	0.036	0.002	0.967	20.516	0.018
50	0.671	0.011	0.005	0.974	46.579	0.079
100	1.765	0.006	0.018	0.993	45.344	0.131
C_o (mg/L)	**$k_{id,1}$ (mg/g $min^{1/2}$)**	**I_1 (mg/g)**	**R^2**	**$k_{id,2}$ (mg/g $min^{1/2}$)**	**I_2 (mg/g)**	**R^2**
25	0.015	-0.033	0.990	0.008	0.005	0.919
50	0.024	0.010	0.977	0.016	0.215	0.999
100	0.161	-0.490	0.996	0.030	0.853	0.943

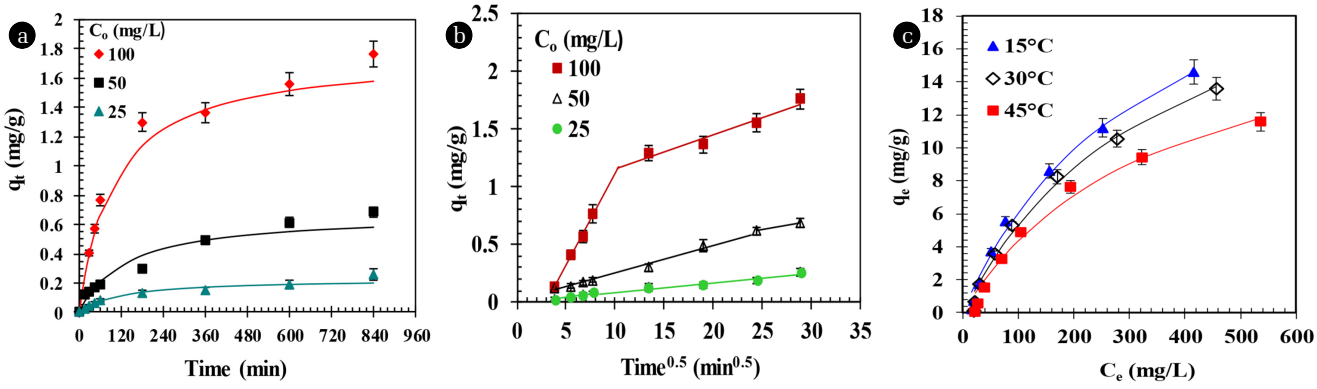

Fig. 1. (a) Effect of contact time on the adsorption of HQ by Fe-GAC, Experimental data plots are given by the symbols and the lines predicted by the pseudo-second order model, T = 30℃, w = 40 g/L. (b) Weber and Morris intra-particle diffusion plot for the removal of HQ by Fe-GAC. T = 30℃, w = 40 g/L. (c) Equilibrium adsorption isotherms at different temperature for HQ by Fe-GAC System t = 14 h, 25-1,000 mg/L, w = 40 g/L. Experimental data points are given by the symbols and the lines predicted by Langmuir isotherm.

rate parameters ($k_{id,1}$ and $k_{id,2}$ shown in Table 2) which are measured from the slope of the q_t versus $t^{1/2}$ plots. First-linear section the gradual equilibrium stage with intra-particle diffusion dominating whereas the second section depicts the final equilibrium stage in which the intra-particle diffusion slow down due to the low HQ left in the solution. Values of $k_{id,1}$ and $k_{id,2}$ are higher for higher C_o indicating enhanced diffusion of HQ through meso- and micro-pores owing to greater driving force at higher C_o. Overall, the intra-particle diffusion of HQ into micro-pores (second section) is the rate controlling step with $k_{id,2}$≈ 0.008-0.030 mg/g $min^{0.5}$) at all C_o. The intercepts of the plots (values of I in Table 2) provide information regarding the boundary layer thickness. Since the value of I are not equal to zero, it indicates that the adsorption proceeds via a complex mechanism consisting of both surface adsorption and intra-particle transport of HQ within the pores of Fe-GAC.

Boyd et al. [53] model incorporating Vermeulen's approximation [54] was used for kinetic data to calculate the effective diffusion coefficient (D_e) by using following equation:

$$\ln\left[\frac{1}{(1-F^2(t))}\right] = \frac{\pi^2 D_e t}{R_a^2} \quad (4)$$

where, $F(t) = q_t/q_e$ and adsorbent particle radius is R_a which is assumed to be spherical (m). The average value of D_e calculated was to be 5.7 × 10^{-14} m^2/s.

As the T increased from 15 to 45°C, the HQ adsorption capacity of Fe-GAC decreased for C_o = 25-1,000 mg/L, w = 40 g/L, t = 14 h and pH_o = 4 (Fig. 1(c)). Therefore, HQ adsorption over Fe-GAC is exothermic in nature indicating that the adsorption of HQ onto Fe-GAC is by physical adsorption. Langmuir, Freundlich and Temkin adsorption isotherms were fitted to experimental data [55-58]. Table 3 shows the isotherms constants obtained for various isotherm models. Langmuir isotherm was found to best represent the experimental data and its fit is shown in Fig. 1(c) by solid lines.

Table 3. Isotherms Parameter for the Removal of HQ by Fe-GAC (t = 14 h, C_o = 25-1,000 mg/L, w = 40 g/L, T = 15-45°C)

Langmuir isotherm	**15°C**	**30°C**	**45°C**
K_L (L/mg)	0.0029	0.0028	0.0028
q_m (mg/g)	26.55	24.47	19.64
R^2	0.985	0.984	0.986
SSE	2.321	2.445	2.801
Chi square (χ^2)	6.000	12.499	22.397
Freundlich isotherm			
K_F ((mg/g)/(mg/L)$^{-1/n}$)	0.222	0.245	0.186
1/n	0.702	0.662	0.669
R^2	0.976	0.979	0.970
SSE	5.871	3.515	7.069
Chi square (χ^2)	11.18	12.790	37.090
Temkin isotherm			
B_T (mg/g)	4.376	4.160	3.667
K_T (L/mg)	0.053	0.047	0.042
R^2	0.989	0.992	0.991
SSE	3.211	1.995	0.897
Chi square (χ^2)	3.513	1.402	3.149

van't Hoff equation (Eq. (5)) gives the correlation between Gibbs free energy (ΔG^o), change in entropy (ΔS^o), the heat of adsorption (ΔH^o) and $K = q_e/C_e$ (called linear adsorption distribution coefficient).

$$\ln K = -\frac{\triangle G^o}{RT} = \frac{\triangle S^o}{R} - \frac{\triangle H^o}{RT} \quad (5)$$

where, R is 8.314 J/mol K and $K = q_e/C_e$ is called linear adsorption distribution coefficient. For significant adsorption, ΔG^o must be negative. The value of ΔG^o at 288 K, 303 K and 318 K were calculated to be −5.5 kJ/mol, −4.2 kJ/mol and −3.6 kJ/mol, respectively. Values of ΔH^o and ΔS^o were calculated to be –23.5 kJ/mol and –63.1 kJ/mol K, respectively. Negative value of ΔH^o confirms exothermic nature of HQ adsorption onto Fe-GAC.

3.2. Catalytic Oxidation Studies

Results of experiments carried out using process parameters as per the L_9 OA are given in Table 1. It has been found that each of the parameters: C_o, pH, C_{H2O2} and m significantly affect the HQ removal efficiency. Individually, at level 1 and 2, C_{H2O2} and pH have the most influence, whereas at level 3, m has the highest influence. It seems that pH has strongest influence over other parameters for the HQ removal from aqueous solution by catalytic oxidation.

HQ removal response curves for the specific effects of various parameters are shown in Fig. 2. As we increase the levels of factors (for example C_o, pH, and m) from 1 to 2, the HQ removal increased. Further increase in the level from 2 to 3 decreased the HQ removal efficiency for the parameters pH, C_{H2O2} and m. ANOVA results for HQ removal efficiency are given in Table S1. To increase the statistical significance of important factors,

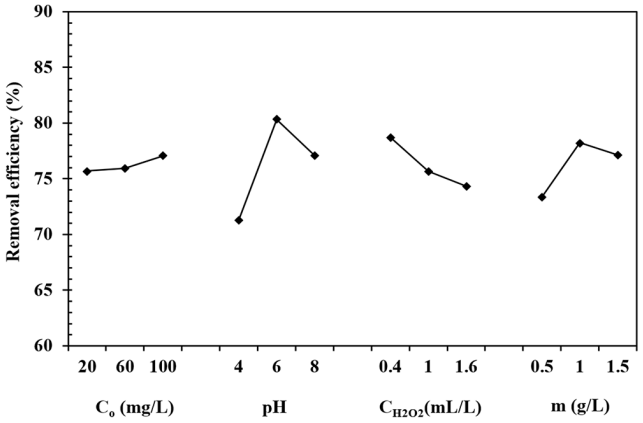

Fig. 2. Effect of process parameter on HQ oxidation by Fe-GAC as computed using Taguchi methodology.

factors with small variance should be pooled. Since factor A has the smaller variance among all factors, therefore it is pooled. After pooling A, ANOVA table is given in Table S2. It is confirmed from Table S2 that the parameter B (pH) is the most influencal factor with 61.89% contribution followed by parameter m (D) with 18.14% contribution.

Since the characteristic of removal efficiency is 'higher-the-better' type, highest value of removal efficiency as shown in the response curves (Fig. 2) is considered to be the optimal. Removal efficiency is higher at level 3 and level 2 for the parameter A and B so that corresponding value is taken as optimum value. Similarly, for parameter C and D, level 1 and level 2 are optimum level for the removal efficiency.

The predicted removal efficiency at optimum levels is 85.62% which is close enough to confirmation experiment which gives the 83.56%. Optimal values obtained are valid for certain values of process parameters, so that for CI_{POP}: 81.22 < removal efficiency < 90.01 and for CI_{CE}: 80.54 < removal efficiency < 90.69.

3.3. Characterization of Fe-GAC

The detailed physico-chemical characterization of Fe-GAC is shown in Table 4. The bulk density of the Fe-GAC was found to be 627 kg/m^3. The proximate analysis showed that Fe-GAC contains 4.5% moisture, 30.1% volatile materials, 21.2% ash and 44.2% fixed carbon. BET analysis showed that Fe-GAC has 77 m^2/g surface area. Barrett, Joyner and Halenda (BJH) adsorption/desorption surface area of pores in Fe-GAC was found to be 48.8/38.8 m^2/g. The single point total pore volume was found to be 0.057 cm^3/g and cumulative BJH adsorption/desorption pore volume was obtained as 0.0425/0.033 cm^3/g in Fe-GAC. The BET and BJH adsorption/desorption average pore diameter were obtained as 29.4 Å and 34.8/33.9 Å, respectively. The structural and morphological characteristics were analyzed by XRD analysis. The broad XRD peak of GAC indicates the presence of amorphous silica. SiO_2 and Fe_2O_3 were found to be the major compounds present in Fe-GAC. XRD did not show any peak conforming crystalline carbon in GAC.

SEM images of GAC, Fe-GAC, Fe-GAC after oxidation of HQ and Fe-GAC after adsorption of HQ are shown in Fig. S3. It may be seen in SEM images that the Fe-GAC has less number of pores

Table 4. Physico-chemical Characteristics of GAC, Fe-GAC, and Fe-GAC after Adsorption of HQ

Characteristic	GAC	Fe-GAC	Fe-GAC after HQ adsorption
Proximate analysis			
Moisture (%)	-	4.5	-
Volatile matter (%)	-	30.10	-
Ash (%)	-	21.21	-
Fixed carbon (%)	-	44.54	-
Bulk density (kg/m^3)	-	627.14	-
Surface area of pores (m^2/g)			
i) BET	137.46	77.29	66.27
ii) BJH			
a) Adsorption cumulative	45.48	48.8	39.42
b) Desorption cumulative	25.38	38.86	27.44
BJH cumulative pore volume (cm^3/g)			
i) single point total	0.082	0.056	0.048
ii) BJH adsorption	0.035	0.042	0.035
iii) BJH desorption	0.015	0.033	0.023
Average pore diameter (Å)			
i) BET	24.13	29.42	29.48
ii) BJH adsorption	31.49	34.85	35.91
iii) BJH desorption	24.08	33.9	33.81

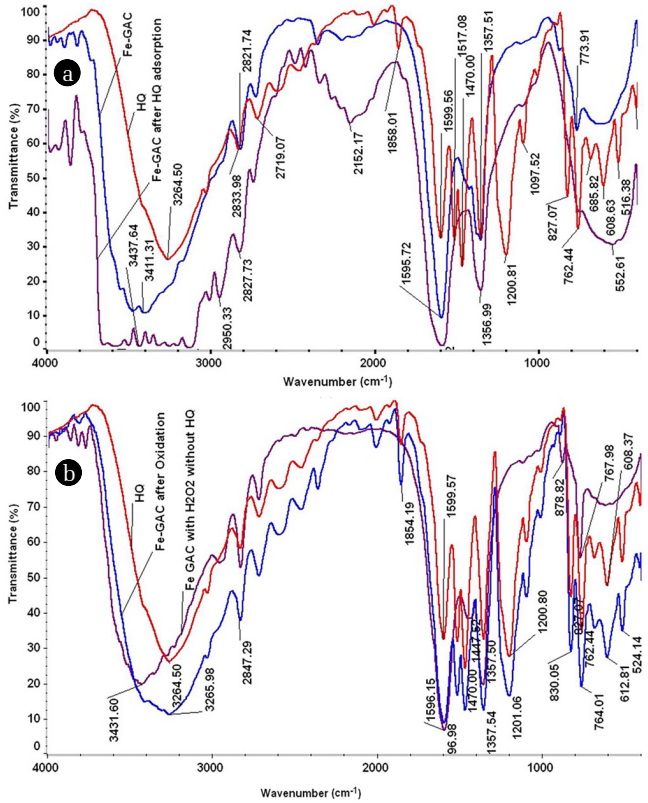

Fig. 3. FTIR of (a) hydroquinone (HQ), Fe-GAC before and after adsorption of HQ; and (b) hydroquinone (HQ), Fe-GAC with H_2O_2 and Fe-GAC after oxidation of HQ.

as compared to that on GAC. It may also be seen that the surface of Fe-GAC get roughened after oxidation, whereas it becomes smoother after adsorption of HQ.

The infrared spectra of HQ, Fe-GAC before and after HQ adsorption are shown in Fig. 3(a). Spectrum of Fe-GAC (Fig. 3(a)) shows a peak at ≈3,420 cm^{-1} representing the presence of OH groups bonded to hydrogen and in free state. Fe-GAC spectrum also displays broad peak at 1,600 cm^{-1} confirming the stretching vibration of CO group because of aldehydes and ketones and due to carbonyl groups bonded to conjugated hydrocarbon.

The FTIR spectrum of HQ and HQ-loaded Fe-GAC show comparable spectra with minor alterations in peak positions and strength. O-H stretching is observed at 3,264 cm^{-1} whereas C-H stretching from aromatic ring is observed at 2,950 and 2,719 cm^{-1}. C-C- stretching is seen at 1,517 cm^{-1} whereas O-H bending is seen at 1,380 cm^{-1} and C-O stretching at 1,200 cm^{-1}. C-H bending is observed at 762 cm^{-1} [59]. It may be seen that few new bands appeared in HQ-adsorbed Fe-GAC and many bands initially existing in blank Fe-GAC were shifted. The transmittance of some of the bands, like for OH stretching, decreased after the adsorption of HQ suggesting the adsorptionof HQ onto Fe-GAC [48].

Fig. 3(b) shows FTIR spectrum for things: (i) for pure HQ, (ii) for Fe-GAC obtained after agitation with H_2O_2 only without HQ and (iii) for Fe-GAC obtained after HQ oxidation with H_2O_2. Comparison of spectra of Fe-GAC obtained after agitation with H_2O_2 only (Fig. 3(b)) with the spectra of blank Fe-GAC (Fig. 3(a)) shows that the peaks related to OH group have shifted towards higher wave numbers and that their transmittance has decreased showing incorporation OH groups onto Fe-GAC because of H_2O_2. However, FTIR spectrum of Fe-GAC obtained after HQ oxidation along with H_2O_2 shows that the transmittance of most of the

peaks has decreased and that this spectrum has lot of similarity with the FTIR spectrum of OH peaks in Fe-GAC obtained after agitation with H_2O_2 only. It seems that H_2O_2 not only helps in the HQ oxidation by OH radical formation but also it adds OH groups onto Fe-GAC. These groups further attract the HQ degradation products onto Fe-GAC, some of which get adsorbed onto Fe-GAC.

3.4. Mechanisms of HQ Adsorption and Catalytic Oxidation

The HQ adsorption onto Fe-GAC occurs through combination of π-π interactions [46], hydrogen-bonding [60, 61] and donor-acceptor interactions. Hydroxyl group, helps in improving the π -donating strength of the aromatic ring because it is an electron-donating functional group. Thus, two -OH groups in HQ helps to increase the HQ adsorption affinity to the Fe-GAC surfaces [47, 62]. Adsorption of HQ on Fe-GAC was due to the electro-chemical interaction between the HQ and the Fe oxides as well as by the active functional groups such as the carboxylic and hydroxide groups present on Fe-GAC [61, 63, 64].

Various types of radicals like hydroxyl (HO•) and hydroperoxyl (HOO•) which play important role in the oxidation of HQ are

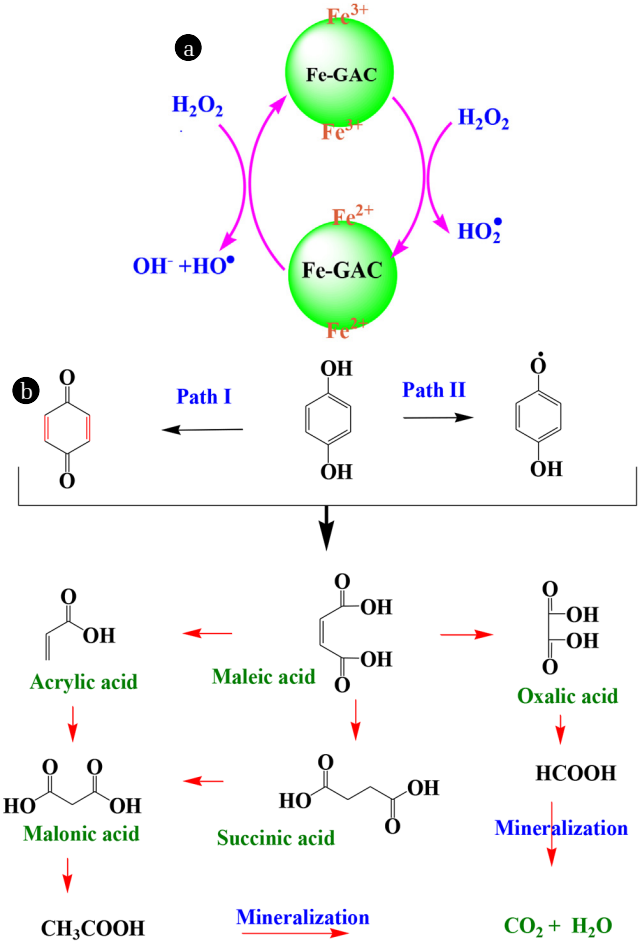

Fig. 4. (a) Hydroxyl radical generation mechanism, (b) Proposed reaction mechanism of hydroquinone degradation.

generated by oxidation-reduction reactions of various iron valences (Fe(III)/Fe(II)) present on the Fe-GAC catalyst in presence of hydrogen peroxide. The oxidation reaction gets started by formation of complex between H_2O_2 and Fe(III)-OH groups [37, 38]. Mechanisms of generation of these radicals represented in Fig. 4(a). These radicals oxidize HQ (i) adsorbed on the catalysts, (ii) present in the vicinity of the catalyst and (iii) in the bulk solution [65, 66]. The HQ oxidation mechanism is shown in Fig. 4(b). HQ, during its oxidation forms various intermediates depending upon the stage of oxidation. It forms intermediates such benzoquinone during early stages of oxidation which get oxidized into acids such as maleic acid, oxalic acid, acrylic acid, succinic acid, malonic acid, acetic acid and formaic acid in the later stage of oxidation; and CO_2 and H_2O upon full oxidation [67, 68].

3.5. Comparison of Adsorption and Catalytic Oxidation Process

Finally, a comparison of HQ removal by catalytic oxidation and adsorption by Fe-GAC can be done. Using catalytic oxidation process, maximum removal efficiency of ~84.5% was observed for C_o = 100 mg/L at pH = 6, m = 1.5 g/L, C_{H2O2} = 0.4 mL/L, T = 50℃ and t = 4 h, whereas, for adsorption, removal efficiency was ~75% with optimum experimental condition being: T = 30℃, pH = 4, t = 10 h and m = 10 g/L. Overall catalytic oxidation seems to better as compared to adsorption. In the catalytic oxidation process, amount of Fe-GAC used is less as compared to adsorption, however, it requires minor amount of H_2O_2 for initiating the oxidation reactions. Moreover, initial pH required in the catalytic oxidation technique is near to neutral pH and the natural pH, thus it can be done without pH adjustment thus not requiring acid for initial pH adjustment. Catalytic oxidation requires higher temperature that will require some energy to be incurred on heating of the solution; however, time required for treatment by catalytic oxidation process is also less than half of that required by the adsorption. Considering the fact that the HQ degrades during the catalytic oxidation process whereas it only gets separated from the solution and gets adsorbs on the Fe-GAC during the adsorption process which will require further disposal of the spent Fe-GAC, overall catalytic oxidation seems to be a better technique for treatment of HQ bearing wastewater. Comparison of work reported on HQ adsorption or mineralization by various adsorbents/catalysts is given in Table S3 [47, 69-75]. Again, mineralization of HQ by Fe-GAC is the better method of HQ removal from aqueous solution. This study shows that metal impregnated adsorbents with stable supports such as GAC can be used as catalyst for catalytic oxidation of wastewater; however, more studies are required on development of the oxidation processes to industrial scale.

4. Conclusions

In this article, a comparative study on the use of Fe-GAC as an adsorbent and catalyst for catalytic oxidation of the HQ was performed. Adsorption study shows that adsorption was favorable at low pH and optimum value was found to be 4. The removal efficiency of HQ by adsorption was increased up to 40 g/L after

that it attains a constant value. The adsorption kinetics was represented by the pseudo-second-order kinetic model. Results show that the obtained equilibrium data from experiments followed the Langmuir isotherm model. Catalytic oxidation studies by Taguchi's experimental design and ANOVA analysis show that pH is the highest influencal factor with 63.47% contribution. The Taguchi experimental design method was used in the experimental oxidation studies. The optimum values of parameter C_o, pH, C_{H2O2} and m are 100 mg/L, 6, 0.4 mL/L and 1 g/L, respectively, in the catalytic oxidation studies by Taguchi's methodology. Detailed characterization and FTIR study showed that H_2O_2 not only helps in the HQ oxidation by OH radical formation but also it adds OH groups onto Fe-GAC which further attracts the HQ degradation products onto Fe-GAC during HQ oxidation. Overall comparison of both processes shows that Fe-GAC works better as a catalyst and that the catalytic oxidation process was found to be better for treatment of HQ bearing aqueous solution.

References

1. Suresh S, Srivastava VC, Mishra IM. Adsorption of catechol, resorcinol, hydroquinone, and their derivatives: A review. *Int. J. Energ. Environ. Eng*. 2012;3:1-19.
2. Enguita FJ, Leitão AL. Hydroquinone: Environmental pollution, toxicity, and microbial answers: Review article. *BioMed. Res. Int*. 2013;2013:1-14.
3. Burqaz S, Ozcan M, Ozkul A, Karakaya AE. Effect of hydroquinone on the development of chick embryo. *Drug Chem. Toxicol*. 1994;17:163-174.
4. Lee JS, Yang EJ, Kim IS. Hydroquinone-induced apoptosis of human lymphocytes through caspase 9/3 pathway. *Mol. Biol. Rep*. 2012;39:6737-6743.
5. Sheftel VO. Handbook of toxic properties of monomers and additives. Boca Raton, FL: Lewis Publishers; 1995.
6. Colinas RJ, Burkart PT, Lawrence DA. In vitro effects of hydroquinone, benzoquinone, and doxorubicin on mouse and human bone marrow cells at physiological oxygen partial pressure. *Toxicol. Appl. Pharmacol*. 1994;129:95-102.
7. Prabhakaran DI, Basha CA, Kannadasan, T, Aravinthan P. Removal of hydroquinone from water by electrocoagulation using flow cell and optimization by response surface methodology. *J. Environ. Sci. Health A Toxic. Hazard. Subst. Environ. Eng*. 2010;45:400-412.
8. El-Ashtoukhy E-SZ, El-Taweel YA, Abdelwahab O, Nassef EM. Treatment of petrochemical wastewater containing phenolic compounds by electrocoagulation using a fixed bed electrochemical reactor. *Int. J. Electrochem. Sci*. 2013;8:1534-1550.
9. Anand MV, Srivastava VC, Singh S, Bhatnagar R, Mall ID. Electrochemical treatment of alkali decrement wastewater containing terephthalic acid using iron electrodes. *J. Taiwan Inst. Chem. Eng*. 2014;45:908-913.
10. Enache TA, Oliveira-Brett AM. Phenol and para-substituted phenols electrochemical oxidation pathways. *J. Electroanal. Chem*. 2011;655:9-16.
11. Akai N, Kawai A, Shibuya K. Water assisted photo-oxidation from hydroquinone to p-benzoquinone in a solid Ne matrix. *J. Photochem. Photobiol. A Chem*. 2011;223:182-188.
12. Tudorachea M, Mahalub D, Teodorescuc C, Stand R, Balae C, Parvulescua VI. Biocatalytic microreactor incorporating HRP anchored onmicro-/nano-lithographic patterns for flow oxidation of phenols. *J. Mol. Catal. B Enzym*. 2011;69:133-139.
13. Fortunya A, Fontb J, Fabregat A. Wet air oxidation of phenol using active carbon as catalyst. *Appl. Catal. B Environ*. 1998;19:165-173.
14. Ting WP, Huang YH, Lu MC. Oxidation of 2,6-dimethylaniline by the Fenton, electro-Fenton and photoelectro-Fenton processes. *J. Environ. Sci. Health A Toxic Hazard. Subst. Environ. Eng*. 2011;46:1085-1091.
15. Maggi R, Piscopoa CG, Sartori G, Storaro L, Moretti E. Supported sulfonic acids: Metal-free catalysts for the oxidation of hydroquinones to benzoquinones with hydrogen peroxide. *Appl. Catal. A Gen*. 2012;411:146-152.
16. Owsik I, Kolarz BZ. The oxidation of hydroquinone to *p*-benzoquinone catalysed by Cu(II) ions immobilized on acrylic resins with aminoguanidyl groups: Part 1. *J. Mol. Catal. A Chem*. 2002;178:63-71.
17. Sato M, Inaki Y, Kondo K, Takemoto K. Functional monomers and polymers. XXXV. Oxidation of hydroquinone catalyzed by Cu(II)-polyelectrolyte complexes. *J. Polym. Sci. Polym. Chem*. 1977;15:2059-2065.
18. Radel RJ, Sullivan JM, Hatfleld JD. Catalytic oxidation of hydroquinone to quinone using molecular oxygen. *Ind. Eng. Chem. Prod. Res. Dev*. 1902;21:566-570.
19. Yamashita K, Niehibu Y, Okada I, Tsuda K. Oxidation of hydrophobic hydroquinone by polyvinylpyridine-Cu(II) complex catalyst. *Polym. Bull*. 1989;22:307-310.
20. Isabela CU, Franka S, Josepa F, Azaela F, Agustíb F, Christophe B. Polymer supported copper catalysts for aqueous phenol oxidation. Recents progres en Genie des Procedes, Numéro 94. Paris, France. 2007.
21. Derikvand F, Bigi F, Maggi R, Piscopo CG, Sartori G. Oxidation of hydroquinones to benzoquinones with hydrogen peroxide using catalytic amount of silver oxide under batch and continuous-flow conditions. *J. Catal*. 2010;271:99-103.
22. Gupta VK, Kumar R, Nayak A, Saleh TA, Barakat MA. Adsorptive removal of dyes from aqueous solution onto carbon nanotubes: A review. *Adv. Colloid Interface Sci*. 2013;193-194:24-34.
23. Gupta VK, Saleh TA. Sorption of pollutants by porous carbon, carbon nanotubes and fullerene – An overview. *Environ. Sci. Pollut. Res*. 2013;20:2828-2843.
24. Gupta VK, Atar N, Yola ML, Üstündağ Z, Uzun L. A novel magnetic Fe@Au core-shell nanoparticles anchored graphene oxide recyclable nanocatalyst for the reduction of nitrophenol compounds. *Water Res*. 2014;48:210-217.
25. Gupta VK, Nayak A, Agarwal S, Tyagi I. Potential of activated carbon from waste rubber tire for the adsorption of phenolics: Effect of pre-treatment conditions. *J. Colloid Interface Sci*. 2014;417:420-430.
26. Gupta VK, Nayak A, Agarwal S. Bioadsorbents for remediation of heavy metals: Current status and their future prospects. *Environ. Eng. Res*. 2015;20:1-18.
27. Saleh TA, Gupta VK. Processing methods, characteristics and adsorption behavior of tire derived carbons: A review. *Adv.*

Colloid Interface Sci. 2014;211:93-101.
28. Garten VA, Weiss DE. The quinone-hydroquinone character of activated carbon and carbon black. *Aust. J. Chem*. 1955;8: 68-95.
29. Ghaedi M, Hajjati S, Mahmudi Z, et al. Modeling of competitive ultrasonic assisted removal of the dyes – Methylene blue and safranin-O using Fe_3O_4 nanoparticles. *Chem. Eng. J.* 2015;268: 28-37.
30. Karthikeyan S, Gupta VK, Boopathy R, Titus A, Sekaran G. A new approach for the degradation of high concentration of aromatic amine by heterocatalytic Fenton oxidation: Kinetic and spectroscopic studies. *J. Mol. Liq.* 2012;173:153-163.
31. Lücking F, Köser H, Jank M, Ritter A. Iron powder, graphite and activated carbon as catalysts for the oxidation of 4-chlorophenol with hydrogen peroxide in aqueous solution. *Water Res*. 1998;32:2607-2614.
32. Zazo JA, Casas JA, Mohedano AF, Rodríguez JJ. Catalytic wet peroxide oxidation of phenol with a Fe/active carbon catalyst. *Appl. Catal. B Environ.* 2006;65:261-268.
33. Abussaud B, Asmaly HA, Ihsanullah, et al. Sorption of phenol from waters on activated carbon impregnated with iron oxide, aluminum oxide and titanium oxide. *J. Mol. Liq*. 2016;213: 351-359.
34. Yin CY, Aroua MK, Daud WMAW. Review of modifications of activated carbon for enhancing contaminant uptakes from aqueous solutions. *Sep. Purif. Technol.* 2007;52:403-415.
35. Pereira M, Oliveira L, Murad E. Iron oxide catalysts: Fenton and Fenton-like reactions – A review. *Clay Miner.* 2016;47: 285-302.
36. Andreozzi R, D'Apuzzo A, Marotta R. Oxidation of aromatic substrates in water/goethite slurry by means of hydrogen peroxide. *Water Res*. 2002;36:4691-4698.
37. Lin SS, Gurol MD. Catalytic decomposition of hydrogen peroxide on iron oxide: Kinetics, mechanism, and implications. *Environ. Sci. Technol*. 1998;32:1417-1423.
38. Kwan WP, Voelker BM. Decomposition of hydrogen peroxide and organic compounds in the presence of dissolved iron and ferrihydrite. *Environ. Sci. Technol*. 2002;36:1467-1476.
39. Quintanilla A, Casas JA, Zazo JA, Mohedano AF, Rodriguez JJ. Wet air oxidation of phenol at mild conditions with a Fe/activated carbon catalyst. *Appl. Catal. B Environ*. 2006;62:115-120.
40. IS 1350-1: Methods of test for coal and coke, Part I: Proximate analysis. Bureau of Indian standards, Manak Bhawan, New Delhi, India. 1984.
41. Srivastava VC, Mall ID, Mishra IM. Multi-component adsorption study of metal ions onto bagasse fly ash using Taguchi's design of experimental methodology. *Ind. Eng. Chem. Res*. 2007;46:5697-5706.
42. Srivastava VC, Mall ID, Mishra IM. Optimization of parameters for adsorption of metal ions onto rice husk ash using Taguchi's experimental design methodology. *Chem. Eng. J*. 2008;140: 136-144.
43. Srivastava VC, Patil D, Srivastava KK. Parameteric optimization of dye removal by electrocoagulation using Taguchi methodology. *Int. J. Chem. Reactor Eng.* 2011;9:article A8.
44. Barker TB. Engineering quality by design. New York: Marcel Dekker, Inc.;1990.
45. Suresh S, Srivastava VC, Mishra IM. Adsorptive removal of phenol from binary aqueous solution with aniline and 4-nitrophenol by granular activated carbon. *Chem. Eng. J.* 2011;171: 997-1003.
46. Blanco-Martinez DA, Giraldo L, Moreno-Pirajan JC. Effect of the pH in the adsorption and in the immersion enthalpy of monohydroxylated phenols from aqueous solutions on activated carbons. *J. Hazard. Mater*. 2009;169:291-296.
47. Suresh S, Srivastava VC, Mishra IM. Adsorption of hydroquinone in aqueous solution by granular activated carbon. *J. Environ. Eng*. 2011;137:1145-1157.
48. Choi H-J. Application of surface modified sericite to remove anionic dye from an aqueous solution. *Environ. Eng. Res.* 2017;22:312-319.
49. Olufemi BA, Otolorin F. Comparative adsorption of crude oil using mango (*Mangnifera indica)* shell and mango shell activated carbon. *Environ. Eng. Res*. 2017;22:384-392.
50. Ho YS, McKay G. Pseudo-second order model for sorption processes. *Process Biochem*. 1999;34:451-465.
51. Rameshraja D, Srivastava VC, Kushwaha JP, Mall ID. Quinoline adsorption onto granular activated carbon and bagasse fly ash. *Chem. Eng. J.* 2012;181-182:343-351.
52. Weber WJ, Morris JC. Kinetics of adsorption on carbon from solution. *J. Sanit. Eng. Div. ASCE* 1963;89:31-60.
53. Boyd GE, Adamson AW, Meyers LS. The exchange adsorption of ions from aqueous solution by organic zeolites. II. Kinetics. *J. Am. Chem. Soc*. 1947;69:2836-2848.
54. Vermeulen T. Theory for irreversible and constant-pattern solid diffusion. *Ind. Eng. Chem*. 1953;45:1664-1670.
55. Langmuir I. The adsorption of gases on plane surfaces of glass, mica and platinum. *J. Am. Chem. Soc.* 1918;40:1361-1403.
56. Freundlich HMF. Over the adsorption in solution. *J. Phys. Chem*. 1906;57:385-471.
57. Temkin MI, Pyzhev V. Kinetics of ammonia synthesis on promoted iron catalyst. *Acta Physicochim. URSS* 1940;12:327-356.
58. Redlich O, Peterson DL. A useful adsorption isotherm. *J. Phys. Chem*. 1959;63:1024-1026.
59. Chatterjee IB. Process for the isolation of a major harmful oxidant from cigarette smoke. Patent No.: US 6782891 B2, 2004.
60. Franz M, Arafat HA, Pinto NG. Effect of chemical surface heterogeneity on the adsorption mechanism of dissolved aromatics on activated carbon. *Carbon* 2000;38:1807-1819.
61. Park HS, Koduru JR, Choo KH, Lee B. Activated carbons impregnated with iron oxide nanoparticles for enhanced removal of bisphenol A and natural organic matter. *J. Hazard. Mater.* 2015;286:315-324.
62. Lin D, Xing B. Adsorption of phenolic compounds by carbon nanotubes: Role of aromaticity and substitution of hydroxyl groups. *Environ. Sci. Technol.* 2008;42:7254-7259.
63. Koduru JR, Lingamdinne LP, Singh J, Choo KH. Effective removal of bisphenol A (BPA) from water using a goethite/activated carbon composite. *Process Saf. Environ. Prot*. 2016;103: 87-96.
64. Lingamdinne LP, Chang YY, Yang JK, et al. Biogenic reductive preparation of magnetic inverse spinel iron oxide nanoparticles for the adsorption removal of heavy metals. *Chem. Eng. J.*

2017;307:74-84.
65. Melero JA, Calleja G, Martınez F, Molina R, Pariente MI. Nanocomposite Fe_2O_3/SBA-15: An efficient and stable catalyst for the catalytic wet peroxidation of phenolic aqueous solutions. *Chem. Eng. J.* 2007;131:245-256.
66. Subbaramaiah V, Srivastava VC, Mall ID. Optimization of reaction parameters and kinetic modeling of catalytic wet peroxidation of picoline by Cu/SBA-15. *Ind. Eng. Chem. Res.* 2013;52:9021-9029.
67. Subbaramaiah V, Srivastava VC, Mall ID. Catalytic activity of Cu/SBA-15 for peroxidation of pyridine bearing wastewater at atmospheric condition. *AIChE J.* 2013;59:2577-2586.
68. Chauhan R, Srivastava VC, Hiwarkar AD. Electrochemical mineralization of chlorophenol by ruthenium oxide coated titanium electrode. *J. Taiwan Inst. Chem. Eng.* 2016;69:106-117.
69. Ding C, Li Y, Wang Y, et al. Highly selective adsorption of hydroquinone by hydroxyethyl cellulose functionalized with magnetic/ionic liquid. *Int. J. Biol. Macromol.* 2018;107:957-964.
70. Jiang X, Chen H-Y, Liu L-L, Qiu L-G, Jiang X. Fe_3O_4 embedded ZIF-8 nanocrystals with ultra-high adsorption capacity towards hydroquinone. *J. Alloy. Compd.* 2015;646:1075-1082.
71. Ouachtak H, Akbour RA, Douch J, Jada A, Hamdani M. Removal from water and adsorption onto natural quartz sand of hydroquinone. *J. Encapsul. Adsorpt. Sci.* 2015;5:131-143.
72. Wang W, Pan S, Xu R, Zhang J, Wang S, Shen J. Competitive adsorption behaviors, characteristics, and dynamics of phenol, cresols, and dihydric phenols onto granular activated carbon. *Desalin. Water Treat.* 2015;56:770-778.
73. Wang X, Lu M, Wang H, Pei Y, Rao H, Du X. Three-dimensional graphene aerogels–mesoporous silica frameworks for superior adsorption capability of phenols. *Sep. Purif. Technol.* 2015;153:7-13.
74. Gosu V, Dhakar A, Sikarwar P, Kumar UKA, Subbaramaiah V, Zhang TC. Wet peroxidation of resorcinol catalyzed by copper impregnated granular activated carbon. *J. Environ. Manage.* 2018;223:825-833.
75. Wang Y, Wei H, Zhao Y, Sun W, Sun C. The optimization, kinetics and mechanism of m-cresol degradation via catalytic wet peroxide oxidation with sludge-derived carbon catalyst. *J. Hazard. Mater.* 2017;326:36-46.